Journal of Applied Polymer Science

Effect of Formulation and Processing Conditions on Light Shielding Efficiency of Thermotropic Systems with Fixed Domains Based on UV Curing Acrylate Resins

Andreas Weber,[1] Sandra Schlögl,[1] Katharina Resch[2]

[1]Polymer Competence Center Leoben GmbH, Roseggerstraße 12, 8700 Leoben, Austria

[2]Department Polymer Engineering and Science, Materials Science and Testing of Polymers, University of Leoben, Otto Glöckel-Straße 2, 8700 Leoben, Austria

Correspondence to: A. Weber (E-mail: andreas.weber@pccl.at)

ABSTRACT: Within this study relationships between material formulation and processing parameters and the morphology (vacuole formation) of thermotropic systems with fixed domains (TSFD) for overheating protection purposes were investigated. Main aim was on improving light shielding efficiency of TSFD based on UV curable acrylate resins by optimization of selected key parameters including photo-initiator type and content, type of reactive diluent, radiation intensity/dose, and thermal treatment of layers during manufacturing. Variations of type of reactive diluent and thermal treatment had a minor effect on overheating protection performance. Utilization of photo-bleaching photo-initiator of acylphospine oxide type instead of a blend of conventional Type I (α-hydroxy ketone type) and Type II (benzophenone) photo-initiators enabled reduction of radiation dose to achieve properly cured layers. The results revealed that a significant reduction of radiation intensity/dose prevented formation of vacuoles. Consequently, light shielding efficiency of TSFD was enhanced significantly. Nevertheless, obtained scattering domain size was inappropriate for optimum light shielding efficiency and requires further optimization strategies. © 2013 Wiley Periodicals, Inc. J. Appl. Polym. Sci. 130: 3299–3310, 2013

KEYWORDS: light scattering; morphology; optical and photovoltaic applications; optical properties; photochemistry

Received 28 February 2013; accepted 23 May 2013; Published online 14 June 2013
DOI: 10.1002/app.39571

INTRODUCTION

Thermotropic glazings providing efficient overheating protection for buildings and solar thermal collectors undergo a transmittance reduction upon exceeding the threshold temperature, reversibly.[1–5] Besides other classes of thermo-responsive glazing materials, thermotropic systems with fixed domains (TSFD) gained interest in recent research due to their specific advantages like high reversibility, low hysteresis, ease of adjustment of switching threshold, high long-term stability, and steep switching process.[6–19] TSFD consist of a thermotropic additive finely dispersed in a matrix material.[1,5] Refractive index difference of matrix and additive and TSFD morphology are of paramount importance for scattering performance and thus overheating protection performance.[20] Refractive indices of matrix and additive are almost equal below the phase transition temperature (e.g., melting temperature) of the additive yielding transparent appearance of the TSFD.[1] Upon exceeding the switching threshold the refractive index difference between matrix and additive increases steeply resulting in a reduction of solar hemispheric transmittance.[1] Maximum light shielding efficiency is attained by spherical scattering domains with diameters in the range between 200 and 400 nm.[20]

The most systematic and extensive study on TSFD so far was performed by Weber et al.[17,18] In total seven different matrix materials (three thermoplastics, four UV-curable resins systems) and 24 different additives were included. More than 40 material formulations were produced and characterized comprehensively based on sound polymer physical principles. Parameters such as refractive index, light shielding efficiency, and morphology were investigated. Fundamental structure-property-relationships were established and material optimization potential and strategies were revealed. From a theoretical point of view thermo-refractive properties of matrix and additive were sufficient in order to achieve a significant reduction of solar hemispheric transmittance upon exceeding the threshold temperature.[17,21] However, investigations revealed inappropriate size and/or shape of scattering domains for achieving optimum light shielding efficiency.[18] Accordingly, overheating protection performance of investigated TSFD was limited.[17,18] Moreover, several TSFD displayed vacuoles at the perimeter of scattering domains, which were adversely affecting overheating protection performance: the vast majority of TSFD exhibiting vacuoles showed an increase in solar hemispheric transmittance upon switching.[17,18] The

high refractive index difference between matrix ($n = 1.5$) and vacuole ($n = 1$) along with small size of vacuoles yielded intense scattering and thus low solar hemispheric transmittance at room temperature. Upon heating and especially upon melting the additive expanded and filled the cavity provided by the matrix material. Thus vacuoles disappeared and a decrease in refractive index difference at the scattering interface (matrix/molten additive) was achieved. Consequently, solar hemispheric transmittance was high above the switching threshold due to lower overall scattering. Details regarding this effect addressed as "effect of the temporary vacuoles" are available from a preceding publication.[18]

Thus, the major objective of the present study is to investigate the relationships between material formulation and processing parameters and the morphology (vacuole formation) of TSFD, in order to improve the light shielding efficiency. Effects are investigated by factorial design. Focus is on TSFD produced from UV curing acrylate systems. TSFD based on thermoplastics are not covered within this study, because of limited feasibility of varying processing conditions.[18]

VACUOLE PREVENTION STRATEGIES

In TSFD with UV-curable resin matrix, vacuole formation is ascribed to thermo-mechanical effects of different coefficients of thermal expansion (CTE) of matrix and additive and limited adhesion at the interface matrix/additive.[18,19] Reduction of irradiation intensity and dose would possibly prevent radiation induced heating up of matrix material and thus vacuole formation.[18] However, reduction of radiation intensity might decrease the final degree of conversion of the matrix resin and thus may yield partially uncured layers.[22]

Hence, more efficient curing would be required. Efficient curing means to decrease radiation dose and yet achieve properly cured layers. A feasible way to increase efficiency of curing process would be the use of photo-bleaching photo-initiator. A photo-bleaching initiator species absorbing at the initiation wavelength is destroyed upon irradiation.[23,24] Thus incident radiation can successively penetrate deeper into the layer, yielding a steady progress of polymerization front towards deeper lying sections of the layer.[23,24] In contrast, according to Lambert–Beer Law, in systems with conventional photo-initiator intensity of radiation at initiation wavelength decreases steadily throughout the layer thickness due to absorption. Hence, more energy is required than for systems formulated with photo-bleaching photo-initiator in order to achieve properly cured layers. Thus, especially for thick layers, photo-bleaching photo-initiators are more efficient (faster and higher conversion) than conventional photo-initiators.[23–26]

For laminate systems with the UV-curable resin between two glass panes, similar to the curing setup in this and preceding studies,[17–19] Decker et al.[27,28] demonstrated a significant effect of glass induced filtering (wavelengths below 330 nm extincted) on conversion profiles of a polyurethane acrylate resin depending on the photo-initiator utilized. Because of filtering of incident radiation by the glass cover, utilization of photo-initiators absorbing above 330 nm is recommended.[27,28] When compared to a conventional α-hydroxyketone initiator (Irgacure 184) an acylphospine oxide photo-initiator (Lucirin TPO) gives superior curing response in a polyurethane acrylate resin laminated between glass panes due to better absorption characteristic upon exposure to filtered UV-light.[27] Thus, regarding production of TSFD, better absorption characteristics when exposed to filtered UV-light and more effective polymerization initiation (more photo-initiator decomposition, less dissipative heat generation by initiator fragments) of photo-bleaching photo-initiator would allow for reduction of irradiation intensity and dose as well as for reduction of initiator content. That probably benefits a reduction of radiation induced heating up of the layers upon curing. However, as photo-initiator is only one out of many chromophores within the resin matrix, experiments have to prove the positive effect of reducing photo-initiator content on dissipative heating and thus vacuole formation.

An alternative approach to inhibit vacuole formation might be minimizing differences in CTE of matrix and additive. Because of lower CTE of matrix material as compared to thermotropic additive (e.g., $6–8 \times 10^{-5}$ K^{-1} for PMMA[29] vs. $0.7–1.1 \times 10^{-3}$ K^{-1} for paraffin[30]), an increase in matrix CTE is desired. An increase in matrix CTE is probably attained by maintaining higher chain mobility. High chain mobility is achieved at temperatures above glass transition temperature and upon lowering crosslinking density.[29,31] Crosslinking density decreases upon decreasing functionality of reactive diluent.[24,32] In preceding studies[17–19], trifunctional reactive diluent trimethylol propane triacrylate (TMPTA) was utilized for formulation of UV-curable matrix resin. Substitution of TMPTA with either a trifunctional reactive diluent with longer flexible spacers between the individual acrylate moieties than in TMPTA or with a bifunctional reactive diluent (lowering number of reactive sites per reactive diluent molecule) might provide more chain mobility and thus probably affect CTE in the desired way.

Investigations by Resch et al.[9,11] suggest viability of these approaches as a bundle of measures. They manufactured TSFD with UV-curable resin matrix formulated with bifunctional reactive diluent hexanediol diacrylate (HDDA) and paraffin-type additive and cured by low intensity UV-light. The samples lacked vacuoles and displayed a reduction of solar hemispheric transmittance upon exceeding the threshold temperature.[8,9,11,16]

Another idea to manipulate vacuole formation is to apply different thermal treatment on cast layers during processing. Upon storage of cast mixture at temperatures below room temperature prior to curing, thermotropic additive domains may stay in a less expanded state than at room temperature. However, upon irradiation matrix temperature increases more intense than additive temperature and likely exceeds room temperature. Both temperatures cannot equilibrate on the short time scales of radiation induced polymerization (below 30 s) due to low thermal conductivity of polymer and additive. Thus, matrix contracts and thermotropic additive expands upon equilibration to room temperature after curing process. Hence, vacuole formation might be prevented by convergent expansion behavior of matrix cavity and respective additive domain. Moreover, thermal treatment might also affect crystallization process of thermotropic

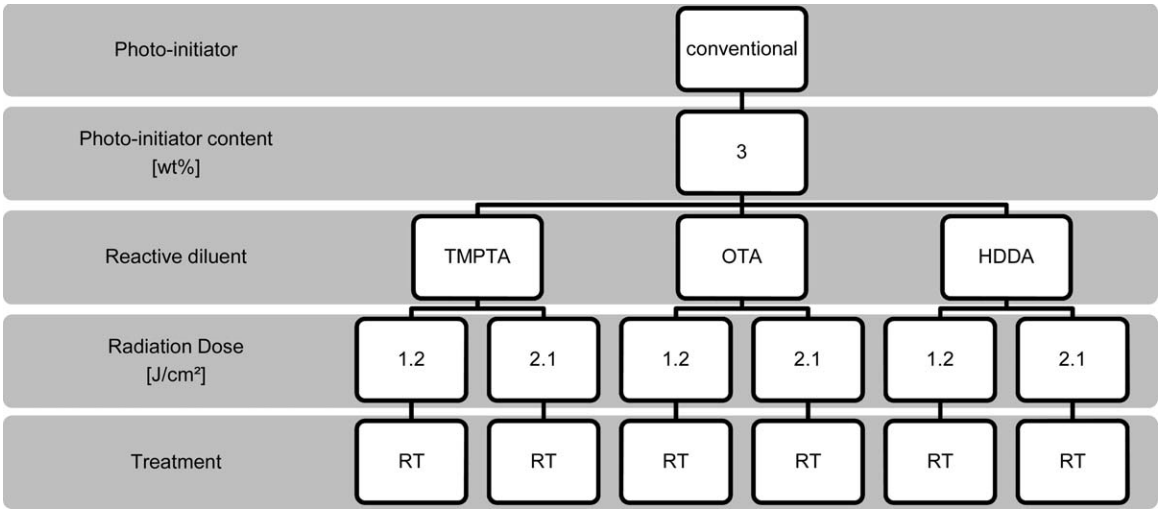

Figure 1. Variations regarding processing conditions and formulation of TSFD (factor levels) formulated with conventional photo-initiator.

additive and hence probably scattering domain size. Mikl[33] demonstrated effects of temperature conditions during manufacturing process on the light shielding efficiency of TSFD. Anyway, information on the morphology of these TSFD was not provided.

Summarizing, factors probably affecting TSFD morphology and being detailed investigated within this study are:

1. Radiation intensity and dose
2. Photo-initiator type and content
3. Type of reactive diluent
4. Thermal treatment during processing

Because of reasons described above (photo-physical processes by chromophores in matrix and photo-initiator, adjusting fit of available radiation and absorption spectrum of photo-initiator) photo-initiator type is assumed to have the most significant effect on morphology of TSFD. Thus, the following experimental part of this article is differentiated by photo-initiator type (conventional photo-initiator and photo-bleaching photo-initiator).

EXPERIMENTAL

Materials and Sample Preparation

Materials. Polyester acrylate oligomer, reactive diluents, and conventional photo-initiator were supplied by Cyctec Surface Specialities. (Drogenbos, B). Photo-bleaching photo-initiator was obtained from BASF SE (Ludwigshafen, D). Paraffin was supplied by Sasol Wax GmbH (Hamburg, D) and HDS-Chemie HandelsgesmbH (Wien, A).

TSFD Formulated with Conventional Photo-Initiator. Figure 1 displays the different formulation and processing parameters applied for TSFD formulated with conventional photo-initiator. Factors varied within these investigations were radiation intensity and dose (factor levels: 0.055 and 0.097 W cm^{-2} yielding 1.2 and 2.1 J cm^{-2}) and type of reactive diluent [factor levels: trimethylolpropane triacrylate (TMPTA), propoxylated glycerol esterified with acrylic acid (OTA), hexanediole diacrylate (HDDA)]. Photo-initiator content and thermal treatment were not varied. Thus, the test design resembles a 2 × 3-mixed level full factorial design. TSFD were manufactured as follows:

A polyester acrylate oligomer was utilized as the major component of the UV-curable resin matrix. Tri functional TMPTA, OTA, and bi functional HDDA were chosen as reactive diluents. Conventional photo-initiator was a blend of benzophenone and 1-hydroxy cyclohexyl phenyl ketone. Thermotropic additive was paraffin with its melting point at 55°C.[17] Thermotropic layers were prepared by dissolving the thermotropic additive in the UV-curable matrix solution consisting of 57 wt % oligomer, 40 wt % reactive diluent, and 3 wt % photo-initiator. Dissolutions were poured in the intervening space between two glass panes, which were sealed around the edge and stored for 10 min at room temperature prior and post curing (treatment RT). Thermotropic mixtures were cured with varying intensities of irradiation and thus doses, either 0.055 or 0.097 W cm^{-2} yielding 1.2 or 2.1 J cm^{-2}, respectively. UV-source was a Light Hammer 6 equipped with a mercury-lamp ("H" bulb) and a LC6E Benchtop Conveyor (Fusion UV Systems, Gaithersburg, MD). Free standing layers with a thickness of 900 μm were obtained after removal of the glass panes. The theoretical additive content was 5 wt %. TSFD were annealed at the mixing temperature of matrix solution and the additive. As to nomenclature, a layer formulated with reactive diluent TMPTA (index "TMPTA"), 3 wt % conventional photo-initiator (index "c3"), applied treatment RT (index "RT") and exposed to a dose of 2.1 J cm^{-2} (index "2.1") is named M7A1-TMPTA-c3-RT-2.1. Because these layers are based on layer M7A1 from preceding publications,[17,18] M7A1 is set as prefix. In Table I the nomenclature of all layers formulated with conventional photo-initiator is presented.

TSFD Formulated with Photo-Bleaching Photo-Initiator. Figure 2 displays the different formulation and processing parameters applied for TSFD formulated with photo-bleaching photo-initiator. Factors varied within the initial investigation were radiation intensity and dose (factor levels: 0.12, 0.39, or

Table I. Nomenclature of TSFD Formulated with Conventional Photo-Initiator

Nomenclature	Reactive diluent	Photo-initiator type	Photo-initiator content (wt %)	Treatment	Dose (J cm^{-2})
M7A1-TMPTA-c3-RT-1.2	TMPTA	Conventional	3	RT	1.2
M7A1-TMPTA-c3-RT-2.1[a]	TMPTA	Conventional	3	RT	2.1
M7A1-OTA-c3-RT-1.2	OTA	Conventional	3	RT	1.2
M7A1-OTA-c3-RT-2.1	OTA	Conventional	3	RT	2.1
M7A1-HDDA-c3-RT-1.2	HDDA	Conventional	3	RT	1.2
M7A1-HDDA-c3-RT-2.1	HDDA	Conventional	3	RT	2.1

[a] Identical with M7A1 from previous publications.[17,18]

0.57 W cm^{-2} yielding 0.6, 2.1, and 3.1 J cm^{-2}), photo-initiator content (factor levels: 1 and 3 wt %) and thermal treatment (factor levels: DF and RT). Type of reactive diluent was not varied. Thus, the initial test design resembled a 3 × 2 × 2-mixed level full factorial design. For in detail investigations, additional factor levels were introduced (see Figure 2). TSFD were manufactured as follows:

A polyester acrylate oligomer and trifunctional reactive diluent OTA along with photo-bleaching photo-initiator (ethyl 2,4,6-trimethylbenzoyl phenyl phosphinate) were utilized for formulation of UV-curable resin matrix. Thermotropic additive was paraffin with its melting point at 55°C.[17] Thermotropic layers were prepared by dissolving the thermotropic additive in the UV-curable matrix solution consisting of 59 or 57 wt % oligomer, 40 wt % reactive diluent and 1 or 3 wt % photo-initiator. Dissolutions were poured in the intervening space between two glass panes, which were sealed around the edge and different thermal treatment was applied prior to curing process. Either the layers were stored at −20°C (treatment DF) or at room temperature (treatment RT) for 10 min prior and post curing. Thermal treatment option HOT (additional factor level not considered initially) was applied for selected systems only as indicated in Figure 2. Upon treatment HOT, the dissolution of molten additive and UV-curable resin were immediately cured after casting process and subsequently stored at room temperature for 10 min after curing. Thermotropic mixtures were cured with varying intensities of 0.12, 0.39, or 0.57 W cm^{-2} from a gallium doped lamp ("V" bulb) of Light Hammer 6, yielding doses of 0.6, 2.1, or 3.1 J cm^{-2}. Additionally, evaluation process required utilization of 366 nm lamp of Universal-UV-lamp (Camag, Muttenz, CH) as UV-source of very low intensity (4.6 μW cm^{-2} yielding 8.3 mJ cm^{-2}; additional factor level). Free standing layers with a thickness of 900 μm were obtained after removal of the glass panes. The theoretical additive content was 5 wt %. TSFD were annealed at the mixing temperature of matrix solution and the additive except for

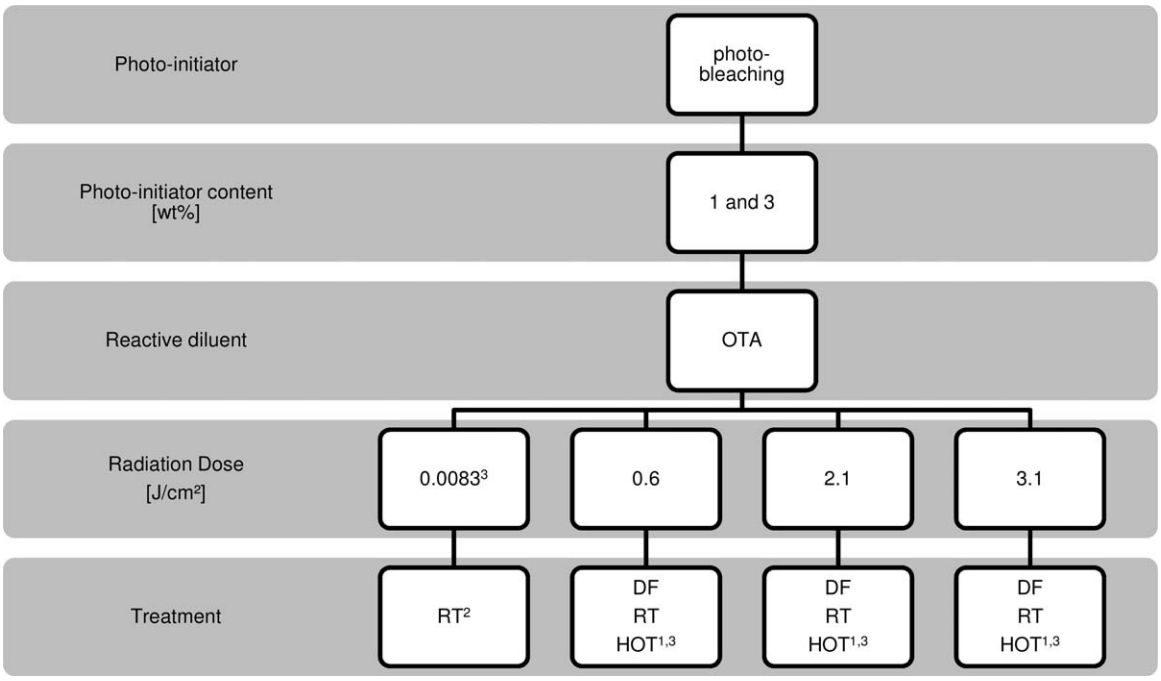

Figure 2. Variations regarding processing conditions and formulation of TSFD (factor levels) formulated with photo-bleaching photo-initiator ([1] for 1 wt % photo-initiator content only;[2] without tempering after curing;[3] additional factor level).

Table II. Nomenclature of TSFD Formulated with 1 wt % Photo-Bleaching Photo-Initiator

Nomenclature	Reactive diluent	Photo-initiator type	Photo-initiator content (wt %)	Treatment	Dose (J cm^{-2})
M7A1-OTA-p1-DF-0.6	OTA	Photo-bleaching	1	DF	0.6
M7A1-OTA-p1-DF-2.1	OTA	Photo-bleaching	1	DF	2.1
M7A1-OTA-p1-DF-3.1	OTA	Photo-bleaching	1	DF	3.1
M7A1-OTA-p1-RT-0.008	OTA	Photo-bleaching	1	RT	0.0083
M7A1-OTA-p1-RT-0.6	OTA	Photo-bleaching	1	RT	0.6
M7A1-OTA-p1-RT-2.1	OTA	Photo-bleaching	1	RT	2.1
M7A1-OTA-p1-RT-3.1	OTA	Photo-bleaching	1	RT	3.1
M7A1-OTA-p1-HOT-0.6	OTA	Photo-bleaching	1	HOT	0.6
M7A1-OTA-p1-HOT-2.1	OTA	Photo-bleaching	1	HOT	2.1
M7A1-OTA-p1-HOT-3.1	OTA	Photo-bleaching	1	HOT	3.1

samples irradiated with Universal-UV-lamp. The latter samples not necessarily required tempering due to rather homogeneous appearance. Furthermore, the effect of tempering on overheating protection performance of TSFD irradiated with Universal-UV-lamp will be addressed in a forthcoming publication. As to nomenclature, a layer formulated with reactive diluent OTA (index "OTA"), 3 wt % photo-bleaching photo-initiator (index "p3"), applied treatment RT (index "RT") and exposed to a dose of 0.6 J cm^{-2} (index "0.6") is named M7A1-OTA-p3-RT-0.6. In Tables II and III the nomenclature of all layers formulated with 1 and 3 wt % photo-bleaching photo-initiator is presented, respectively.

Characterization Methodology

Light Shielding Efficiency. Overheating protection performance of TSFD was determined applying UV/Vis/NIR spectrometry. A double beam UV/Vis/NIR spectrophotometer Lambda 950 (Perkin Elmer, Waltham, MA) equipped with an Ulbricht-sphere (diameter 150 mm) was employed. For the given measurement apparatus the radiation passing through (transmittance) the specimen outside a cone of ~5° relative to the incident beam direction was defined as diffuse (scattered) component. Hemispheric and diffuse transmittance was recorded at normal incidence in the spectral region from 250 to 2500 nm. The integral solar transmittance was determined by weighting the recorded spectral data in steps of 5 nm by the AM1.5 global solar irradiance source function. The spectrophotometer was adapted by a heating stage to adjust sample temperature within a range from ambient temperature to maximum 115°C.[17] Measurements were performed in steps of 5°C. Prior to measurement the samples were allowed to equilibrate for 5 min at the selected temperature. The heating stage was equipped with a control system consisting of a heating stage-internal J-type thermocouple as temperature sensor and the control unit HS-W-35/M (Heinz Stegmeier Heizelemente HS-Heizelemente GmbH, Fridingen, D). Within the heating stage the sample was positioned in close proximity of the port hole of the Ulbricht-sphere. *In situ* front- and backside sample surface temperatures as a function of set-point value of the control unit were recorded on a prototype sample with a two-channel temperature measurement instrument T900 (Dostmann electronic GmbH, Wertheim-Reicholzheim, D) equipped with a precision K-type thermocouple. Sample temperature was assumed as the average of both recorded surface temperatures. Required set-point values to maintain average sample temperatures were calculated from a second order polynomial fit of the temperatures recorded in measurements of the prototype sample.

Morphology. Morphological characterization of TSFD was carried out applying an optical microscope Olympus BX51 (Olympus Austria Ges. m. b. H., Wien, A) in transmitted light mode. TSFD were investigated without further preparation. Domain size was evaluated with measurement tools of software analySIS (Soft Imaging System GmbH, Münster, D). Minimum and maximum sizes of scattering domains were evaluated.

Table III. Nomenclature of TSFD Formulated with 3 wt % Photo-Bleaching Photo-Initiator

Nomenclature	Reactive diluent	Photo-initiator type	Photo-initiator content (wt %)	Treatment	Dose (J cm^{-2})
M7A1-OTA-p3-DF-0.6	OTA	Photo-bleaching	3	DF	0.6
M7A1-OTA-p3-DF-2.1	OTA	Photo-bleaching	3	DF	2.1
M7A1-OTA-p3-DF-3.1	OTA	Photo-bleaching	3	DF	3.1
M7A1-OTA-p3-RT-0.008	OTA	Photo-bleaching	3	RT	0.0083
M7A1-OTA-p3-RT-0.6	OTA	Photo-bleaching	3	RT	0.6
M7A1-OTA-p3-RT-2.1	OTA	Photo-bleaching	3	RT	2.1
M7A1-OTA-p3-RT-3.1	OTA	Photo-bleaching	3	RT	3.1

Applied Polymer SCIENCE

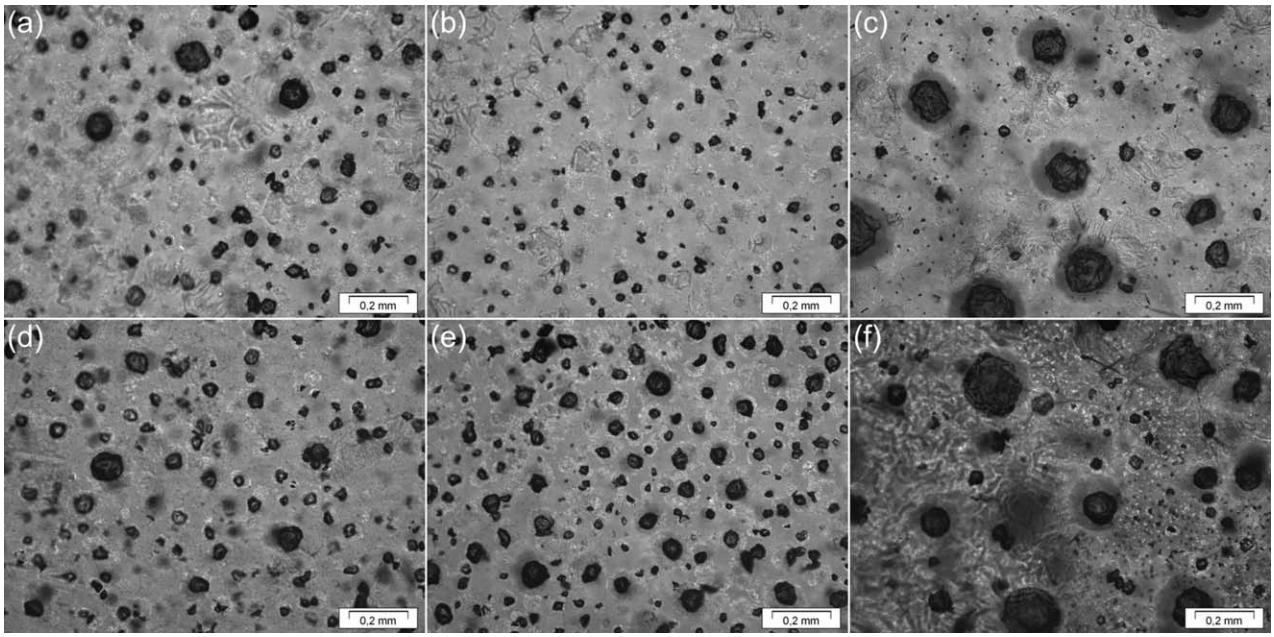

Figure 3. Optical micrographs of TSFD formulated with different reactive diluents and irradiated with different doses from "H" bulb of Light Hammer 6 after storage at room temperature (treatment RT) (a) M7A1-TMPTA-c3-RT-1.2 (b) M7A1-OTA-c3-RT-1.2, (c) M7A1-HDDA-c3-RT-1.2, (d) M7A1-TMPTA-c3-RT-2.1, (e) M7A1-OTA-c3-RT-2.1, and (f) M7A1-HDDA-c3-RT-2.1.

RESULTS AND DISCUSSION

TSFD Formulated with Conventional Photo-Initiator

In Figure 3 the optical micrographs of layers M7A1-TMPTA-c3-RT-1.2 [Figure 3(a)], M7A1-OTA-c3-RT-1.2 [Figure 3(b)], M7A1-HDDA-c3-RT-1.2 [Figure 3(c)], M7A1-TMPTA-c3-RT-2.1 [Figure 3(d)], M7A1-OTA-c3-RT-2.1 [Figure 3(e)] and M7A1-HDDA-c3-RT-2.1 [Figure 3(f)] are presented. Layers exhibited spherical scattering domains with diameters ranging from 1.10 to 150 μm [M7A1-TMPTA-c3-RT-1.2, Figure 4(a)], 3.31 to 85.6 μm [M7A1-OTA-c3-RT-1.2, Figure 4(b)], 1.93 to

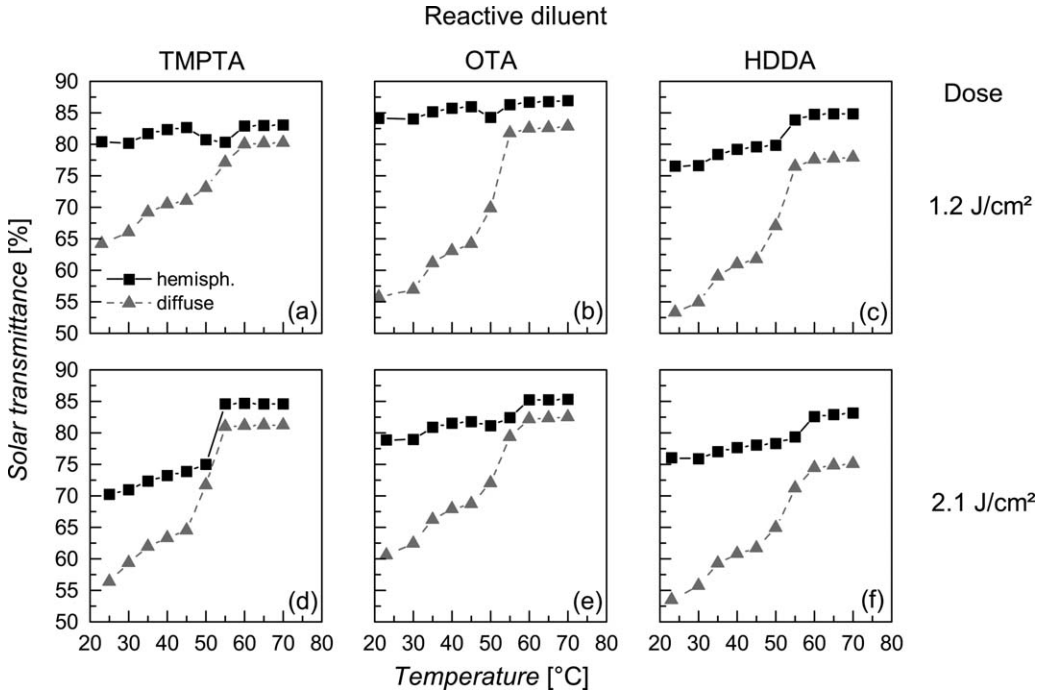

Figure 4. Solar hemispheric and diffuse transmittance as a function of temperature of TSFD formulated with 3 wt % conventional photo-initiator and different reactive diluents, irradiated with different doses from "H" bulb of Light Hammer 6 after storage at room temperature (treatment RT) (a) M7A1-TMPTA-c3-RT-1.2, (b) M7A1-OTA-c3-RT-1.2, (c) M7A1-HDDA-c3-RT-1.2, (d) M7A1-TMPTA-c3-RT-2.1, (e) M7A1-OTA-c3-RT-2.1, (f) M7A1-HDDA-c3-RT-2.1.

229 μm [M7A1-HDDA-c3-RT-1.2, Figure 4(c)], 2.48 to 167 μm [M7A1-TMPTA-c3-RT-2.1, Figure 4(d)], 2.48 to 139 μm [M7A1-OTA-c3-RT-2.1, Figure 4(e)], and 3.86 to 242 μm [M7A1-HDDA-c3-RT-2.1, Figure 4(f)]. For all these layers domain size is inappropriate for efficient overheating protection. Largest domains were ascertained for layers formulated with HDDA. This may be attributed to lower viscosity of dissolutions formulated with HDDA compared to systems formulated with trifunctional TMPTA or OTA. Low viscosity systems probably yield faster aggregation of additive droplets prior to solidification. Furthermore, layers displayed distinct vacuoles at the perimeter of the additive domains (black areas).

A distinct effect of radiation dose and type of reactive diluent on vacuole formation was evident. For layers formulated with HDDA [M7A1-HDDA-c3-RT-1.2 [Figure 4(c)] and M7A1-HDDA-c3-RT-2.1 [Figure 4(f)], no distinct correlation between irradiation dose and vacuole concentration was ascertainable. Nearly every scattering domain exhibited a vacuole. On the contrary, a significant effect of radiation dose on vacuole concentration was observed for layers formulated with TMPTA and OTA: lower irradiation dose yielded a reduction of vacuoles (compare: M7A1-TMPTA-c3-RT-1.2 [Figure 4(a)] and M7A1-TMPTA-c3-RT-2.1 [Figure 4(d)]; M7A1-OTA-c3-RT-1.2 [Figure 4(b)], and M7A1-OTA-c3-RT-2.1 [Figure 4(e)]). As described above, the reduction of irradiation intensity and dose decreases dissipative heating up of the matrix material and may affect vacuole formation. However, irradiation intensity and dose and hence dissipative heating did not affect concentration of vacuoles in layers formulated with HDDA. Because of its moderate curing response bifunctional reactive diluent HDDA is probably not able to fix established structures fast enough, giving the vacuoles sufficient time to establish, independent on temperature. On the contrary, vacuoles were formed to a minor extent upon reduction of irradiation intensity and dose for layers formulated with trifunctional TMPTA or OTA. Besides decreased dissipative heating also, fast curing response of trifunctional reactive diluents, yielding rather fast fixation of established structures, and thus limiting vacuole formation, may positively affect layer morphology.

Figure 4 displays the solar hemispheric (square) and diffuse (triangle) transmittance as a function of temperature of TSFD M7A1-TMPTA-c3-RT-1.2 [Figure 4(a)], M7A1-OTA-c3-RT-1.2 [Figure 4(b)], M7A1-HDDA-c3-RT-1.2 [Figure 4(c)], M7A1-TMPTA-c3-RT-2.1 [Figure 4(d)], M7A1-OTA-c3-RT-2.1 [Figure 4(e)], and M7A1-HDDA-c3-RT-2.1 [Figure 4(f)]. The solar hemispheric transmittance of layers M7A1-TMPTA-c3-RT-1.2, M7A1-OTA-c3-RT-1.2, and M7A1-HDDA-c3-RT-1.2 increased from 80.4, 84.1, and 76.6% at ambient conditions to 83.1, 86.9, and 84.8% at 70°C, respectively. These layers exhibited an increase in solar diffuse transmittance from between 53.3 and 64.2% to values ranging from 77.9 to 82.8% upon heating. The solar hemispheric transmittance of layers M7A1-TMPTA-c3-RT-2.1, M7A1-OTA-c3-RT-2.1, and M7A1-HDDA-c3-RT-2.1 increased from 70.3, 78.9, and 76.1% at ambient conditions to 84.6, 85.3, and 83.1% at 70°C, respectively. These layers exhibited an increase in solar diffuse transmittance from between 53.5 and 60.6% to values ranging from 75.1 to 82.5% upon heating. The observed increase in solar hemispheric transmittance around the switching threshold was ascribed to the effect of temporary vacuoles as already described above. Upon heating also a slight increase in solar hemispheric and diffuse transmittance was detected around 35°C, which is corresponding to solid phase transition of the thermotropic additive.[17] Probably due to expansion of additive upon solid phase transmittance several vacuoles vanish, yielding lower vacuole concentration and thus lower overall scattering performance. Whereas this effect was rather weak upon further heating for solar hemispheric transmittance, solar diffuse transmittance increased steadily. Upon melting of the additive around 55°C,[17] a more or less distinct increase in both, solar hemispheric and diffuse transmittance occurred. This effect was ascribed to disappearance of vacuoles because of expansion of additive upon melting, thus filling the complete domain cavity provided by the surrounding matrix.[18] Accordingly, the scattering domains with inappropriate diameter for back scattering yielded strong forward scattering.

Differences in switching characteristics of these TSFD were attributed to different layer morphology (vacuoles), and hence correlated with radiation intensity and dose applied and type of reactive diluent used. Layers formulated with bifunctional HDDA displayed rather congruent curves of solar hemispheric and diffuse transmittance as a function of temperature. This was ascribed to the invariance of vacuole concentration upon changes in radiation intensity and dose (Figure 3). In contrast, layers formulated with trifunctional TMPTA or OTA displayed a lower solar hemispheric transmittance at room temperature along with a more distinct increase in solar hemispheric transmittance upon switching if irradiated with higher dose. This corresponded well with higher vacuole concentration detected for layers irradiated with 2.1 J cm^{-2} as compared to layers irradiated with 1.2 J cm^{-2} (Figure 3). Among layers formulated with trifunctional reactive diluents (TMPTA and OTA), higher solar hemispheric transmittance was achieved by layers formulated with OTA, irrespective of applied radiation dose and reference temperature (room temperature or 70°C). OTA exhibits longer spacers between vinyl-moieties as compared to TMPTA, thus yielding higher matrix flexibility due to higher chain mobility.

TSFD Formulated with Photo-Bleaching Photo-Initiator

In layers formulated with conventional photo-initiator and with trifunctional reactive diluents TMPTA or OTA a reduction in radiation dose yielded a decrease of vacuole concentration. Hence, the following investigations will also address very low curing intensities. Anyway, as further reduction of radiation dose would yield partially uncured layers, a photo-bleaching photo-initiator will be used. Furthermore, subsequent investigations focus on systems formulated with OTA. Layers formulated with OTA exhibited higher solar hemispheric transmittance than layers formulated with TMPTA (see Figure 4).

Effects of Radiation Dose, Thermal Treatment, and Photo-Initiator Content on Light-Shielding Efficiency. For evaluation of the effects of the factors radiation dose, thermal treatment, and photo-initiator content on light shielding efficiency of

Table IV. Scattering Domain Size in TSFD Formulated with 40 wt % OTA and 3 wt % Photo-Bleaching Photo-Initiator for Different Thermal Treatment Prior to UV-Exposure ("V" Bulb) of the Layers

	Radiation dose					
	0.6 (J cm^{-2})		2.1 (J cm^{-2})		3.1 (J cm^{-2})	
Treatment	d_{min} (μm)	d_{max} (μm)	d_{min} (μm)	d_{max} (μm)	d_{min} (μm)	d_{max} (μm)
DF	2.48	126	1.38	113	1.66	189
RT	1.10	85.6	3.04	224	2.21	144

Table V. Scattering Domain Size in TSFD Formulated with 40 wt % OTA and 1 wt % Photo-Bleaching Photo-Initiator for Different Thermal Treatment Prior to UV-Exposure ("V" Bulb) of the Layers

	Radiation dose					
	0.6 (J cm^{-2})		2.1 (J cm^{-2})		3.1 (J cm^{-2})	
Treatment	d_{min} (μm)	d_{max} (μm)	d_{min} (μm)	d_{max} (μm)	d_{min} (μm)	d_{max} (μm)
DF	1.24	113	1.52	74.5	1.10	142
RT	3.17	95.2	2.07	171	4.42	258
HOT	2.48	86.9	2.76	112	2.62	126

TSFD a test design resembling a mixed level full-factorial design was established. Factor levels were 0.6, 2.1, and 3.1 J cm^{-2} for radiation dose, DF and RT for thermal treatment and 1 and 3 wt % for photo-initiator content, respectively.

Tables IV and V present diameters of spherical scattering domains for layers irradiated with different doses from "V" bulb of Light Hammer 6 (0.6, 2.1, and 3.1 J cm^{-2}) and different thermal treatment (treatment DF and RT) formulated with 3 and 1 wt % photo-initiator content, respectively. In general no effect of photo-initiator content, radiation dose, and thermal treatment on sample morphology was observed (factor levels: DF or RT; 0.6, 2.1, or 3.1 J cm^{-2}). Scattering domain size varied between 1.10 and 258 μm. Furthermore, nearly every scattering domain exhibited a vacuole. Anyway, the scattering domain sizes detected for these layers were inappropriate for efficient overheating protection.

Figure 5 presents the mean plots regarding the factors radiation dose applied from "V" bulb of Light Hammer 6 (0.6, 2.1, and 3.1 J cm^{-2}), photo-initiator content (1 and 3 wt %) and thermal treatment (treatment DF or RT) on solar hemispheric (square symbols) and diffuse transmittance (triangle symbols) of TSFD formulated with reactive diluent OTA. Data were recorded at room temperature RT (solid symbols) and 70°C (open symbols). Mean and standard deviation of solar hemispheric and diffuse transmittance of layers regarding applied radiation dose were calculated by merging data of TSFD M7A1-OTA-p1-DF-0.6, M7A1-OTA-p1-RT-0.6, M7A1-OTA-p3-DF-0.6, and M7A1-OTA-p3-RT-0.6 for a dose of 0.6 J cm^{-2} for example. The mean and standard deviation of solar transmittances regarding other factor levels were calculated accordingly.

As to solar transmittance, three general trends were evident: (1) Solar hemispheric transmittance increased from between 49.4 and 56.0% at ambient temperature to values between 70.3 and 80.8% upon exceeding the threshold temperature. The increase is attributable to the effect of temporary vacuoles. (2) Detected diameters of scattering domains yielded intense forward scattering thus resulting in rather high solar diffuse transmittance of around 47 and 73% at room temperature and 70°C, respectively. (3) Applied radiation dose, thermal treatment, and photo-initiator content do not affect the level of solar transmittance significantly. The invariance against the two factors radiation dose and photo-initiator content was ascribed to the high curing efficiency of the photo-bleaching photo-initiator, yielding fast curing response also upon low intensities and low photo-initiator content. However, invariance against these two parameters also indicated that dissipation of irradiated energy was too high in order to mitigate vacuole formation and thus to achieve a reduction of solar hemispheric transmittance upon heating. The invariance of solar transmittance against photo-initiator

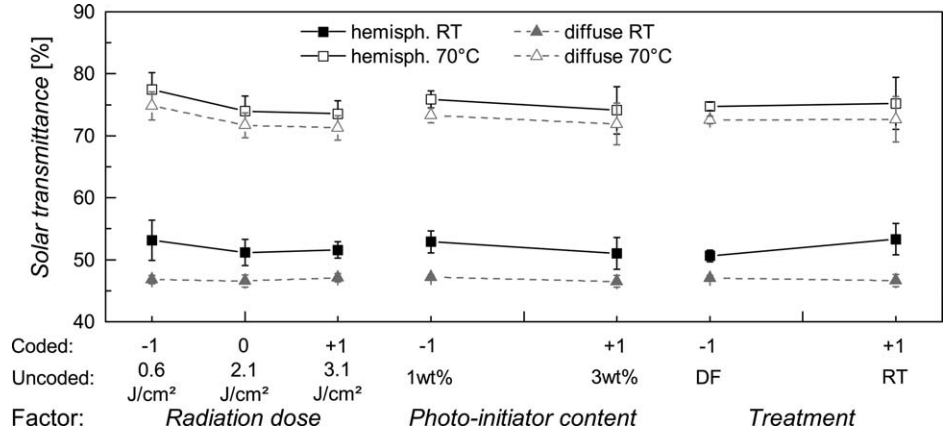

Figure 5. Mean plot regarding effects of factors radiation dose applied from "V" bulb of Light Hammer 6 (factor levels: 0.6, 2.1, and 3.1 J cm^{-2}), photo-initiator content (factor levels: 1 and 3 wt%) and thermal treatment (factor levels: DF: −20°C/10 min prior and post curing; RT: room temperature/10 min prior and post curing) on solar hemispheric and diffuse transmittance of TSFD formulated with reactive diluent OTA and photo-bleaching photo-initiator. Data were recorded at room temperature RT and 70°C, respectively.

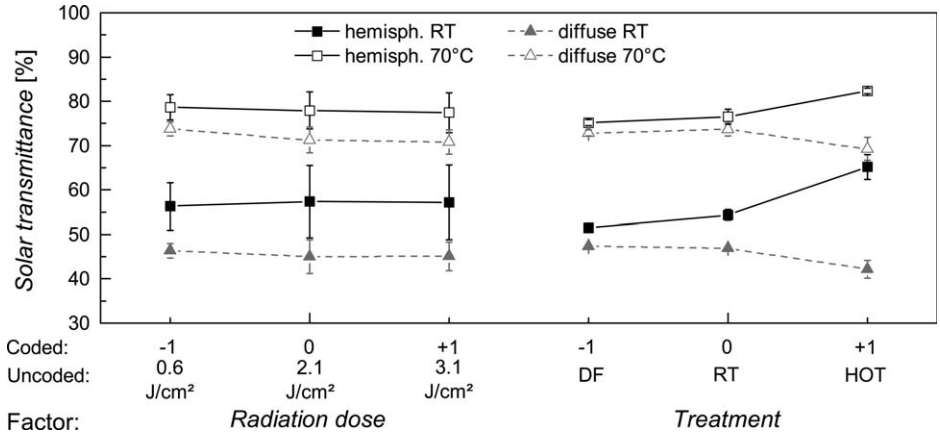

Figure 6. Mean plot regarding effects of factors radiation dose applied from "V" bulb of Light Hammer 6 (factor levels: 0.6, 2.1, and 3.1 J cm^{-2}) and thermal treatment (factor levels: DF: −20°C/10 min prior and post curing; RT: room temperature/10 min prior and post curing; HOT: immediately cured in the hot state after casting, storage at room temperature/10 min post curing) on solar hemispheric and diffuse transmittance of TSFD formulated with reactive diluent OTA and 1 wt % photo-bleaching photo-initiator. Data were recorded at room temperature RT and 70°C, respectively.

content revealed an insignificant contribution of photo-initiator content to overall radiation dissipation. The effect of other chromophores inside the matrix resin is higher.

Upon variation of thermal treatment slight changes in solar transmittances were achieved. Solar hemispheric transmittance at room temperature was slightly higher for treatment RT (53.3 ± 2.5%) than for treatment DF (50.6 ± 0.92%). However, initial considerations anticipated a higher solar hemispheric transmittance at room temperature for layers exposed to treatment DF than for those exposed to treatment RT. Thus, additional investigations regarding this effect are carried out in the subsequent section. Nevertheless, solar diffuse transmittance at room temperature did not vary upon change in thermal treatment (DF: 47.0 ± 0.47%; RT: 46.7 ± 0.97%). This was ascribed to similar scattering domain sizes detected for the respective layers (see Tables IV and V).

At 70°C high solar hemispheric transmittance of 75.0 ± 2.9% was achieved. This was attributed to the absence of vacuoles at this temperature. Solar diffuse transmittance was 72.6 ± 2.5%. The high diffuse fraction of the solar hemispheric transmittance was attributed to inappropriate scattering domain size for efficient back-scattering.

Effect of Higher Temperature of Thermal Treatment on Light-Shielding Efficiency. The variation of thermal treatment revealed a slight effect on solar hemispheric transmittance (see above). Thus in the following an additional factor level is evaluated for this factor. Because of invariance of solar hemispheric transmittance upon changes in photo-initiator content, layers formulated with 1 wt % photo-bleaching photo-initiator were chosen as model system (see Figure 2). Hence, this test design resembles a 3 × 3 full factorial design.

Table V presents diameters of spherical scattering domains detected for layers irradiated with different doses from "V" bulb of Light Hammer 6 (0.6, 2.1, and 3.1 J cm^{-2}) and different thermal treatment (treatment DF, RT, and HOT) formulated with 1 wt % photo-initiator. In general no effect of radiation dose and thermal treatment on sample morphology was observed (factor levels: DF, RT, or HOT; 0.6, 2.1, or 3.1 J cm^{-2}). Scattering domain size varied between 1.10 and 258 μm. Furthermore, nearly every scattering domain exhibited a vacuole. Anyway, the scattering domain sizes detected for these layers were inappropriate for efficient overheating protection.

Figure 6 presents the mean plots regarding the factors radiation dose applied from "V" bulb of Light Hammer 6 (0.6, 2.1, and 3.1 J cm^{-2}) and thermal treatment (treatment DF, RT, and HOT) on solar hemispheric (square symbols) and diffuse transmittance (triangle symbols) of TSFD formulated with reactive diluent OTA and 1 wt % photo-bleaching photo-initiator. Data were recorded at room temperature RT (solid symbols) and 70°C (open symbols).

Solar transmittances did not vary upon changes in radiation dose (Figure 6). Solar hemispheric transmittance was around 57 and 78% at room temperature and 70°C, respectively. Solar diffuse transmittance was around 45 and 72% at room temperature and 70°C, respectively. The observed increase in solar hemispheric and diffuse transmittance upon heating was attributed to the effect of temporary vacuoles. The high diffuse fraction of solar hemispheric transmittance was ascribed to inappropriate scattering domain size for efficient back-scattering.

In contrast, thermal treatment applied during manufacturing affected solar hemispheric transmittance significantly. With increasing treatment temperature (order DF < RT < HOT) solar hemispheric transmittance increased. At room temperature solar hemispheric transmittance of 51.4, 54.3, and 65.2% were detected for factor levels DF, RT, and HOT, respectively. At the same time a solar diffuse transmittance of 42.2% at room temperature was evident for treatment HOT. Treatments DF and RT yielded a solar diffuse transmittance of 47.4 and 46.9% at room temperature, respectively.

Deviant from what was expected (see section "Vacuole prevention strategies"), the actually detected level of solar hemispheric transmittance at room temperature was in the order DF < RT < HOT. Observed order indicates that layers exposed to treatment HOT probably exhibited a bigger average size of vacuoles

Applied Polymer SCIENCE

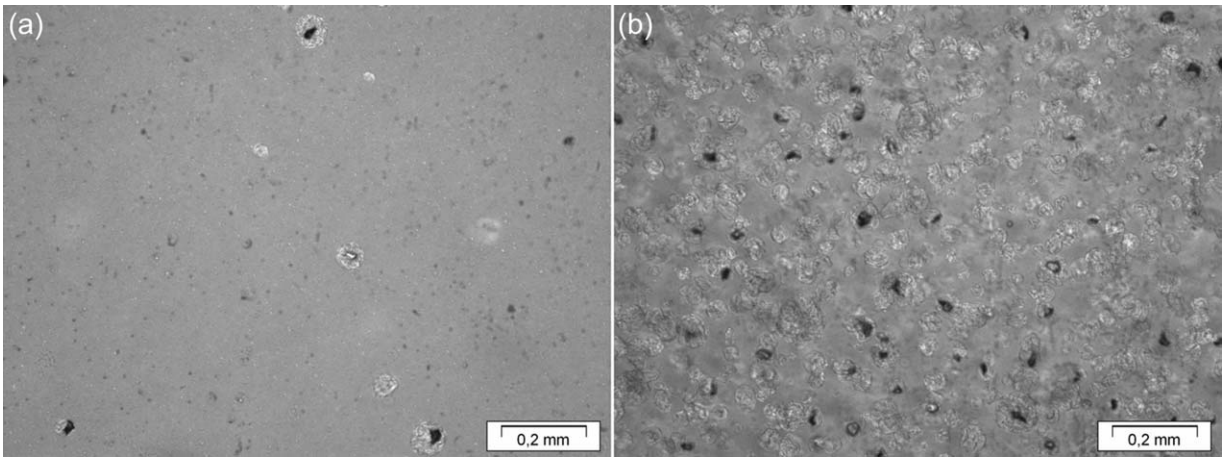

Figure 7. Optical micrographs of TSFD formulated with reactive diluent OTA and either (a) 1 wt % or (b) 3 wt % photo-bleaching photo-initiator and irradiated with Universal-UV-lamp after storage at room temperature (treatment RT).

yielding less efficient back-scattering. That might be due to a more left-tailed size distribution of scattering domains for layers exposed to treatment HOT, yielding a more left tailed size distribution of vacuoles as compared to layers exposed to treatment DF or RT. Hence, the actually detected order was likely due to lower back-scattering efficiency of bigger vacuoles.

These trends were also observed for solar transmittances recorded at 70°C. Solar hemispheric transmittance was 75.2, 76.5, and 82.3% for treatments DF, RT, and HOT, respectively. The enhanced solar hemispheric transmittance at 70°C for treatment HOT as compared to treatments DF and RT was probably a side effect of the vacuole size distribution issue. Maybe not all vacuoles disappeared upon exceeding the threshold temperature for treatments DF and RT, thus yielding residual back scattering. At the same time solar diffuse transmittance was 72.9, 73.7, and 69.3% for treatments DF, RT, and HOT, respectively. This was probably due to a reduced concentration of larger scattering domains in layers exposed to treatment HOT as compared to layer exposed to treatments DF or RT.

Effect of Reduced Irradiation Intensity on Light-Shielding Efficiency. The results achieved so far indicate that temperature difference between matrix and additive is probably the most crucial parameter affecting light-shielding performance. However, further increasing treatment temperature is not feasible because of deterioration and evaporation of TSFD constituents. Thus, preventing dissipative heating up of the matrix might be more beneficial. Hence, for the following discussion layers formulated with either 1 or 3 wt % photo-bleaching photo-initiator were exposed to radiation of low intensity (4.6 $\mu W\ cm^{-2}$ yielding 8.3 $mJ\ cm^{-2}$) of 366 nm lamp of Universal-UV-lamp. With respect to a potential practical application in future, thermal treatment RT was applied solely (see Figure 2).

Figure 7 displays optical micrographs of the layers M7A1-OTA-p1-RT-0.008 [Figure 7(a)] and M7A1-OTA-p3-RT-0.008 [Figure 7(b)]. The layers displayed spherical scattering domains with diameters ranging from 3.31 to 84.2 μm and from 2.76 to 116 μm for layers formulated with 1 and 3 wt % photo-initiator, respectively. For both layers only few vacuoles were evident at the perimeter of the scattering domains. The vacuole concentration was significantly lower for these TSFD as compared to the layers discussed above (e.g., Figure 3). This was ascribed to the very low irradiation intensity preventing excessive dissipative heating up of the matrix material.

In Figure 8 the solar hemispheric (square) and diffuse (triangle) transmittance of TSFD M7A1-OTA-p1-RT-0.008 [Figure 8(a)] and M7A1-OTA-p3-RT-0.008 [Figure 8(b)] is depicted as a

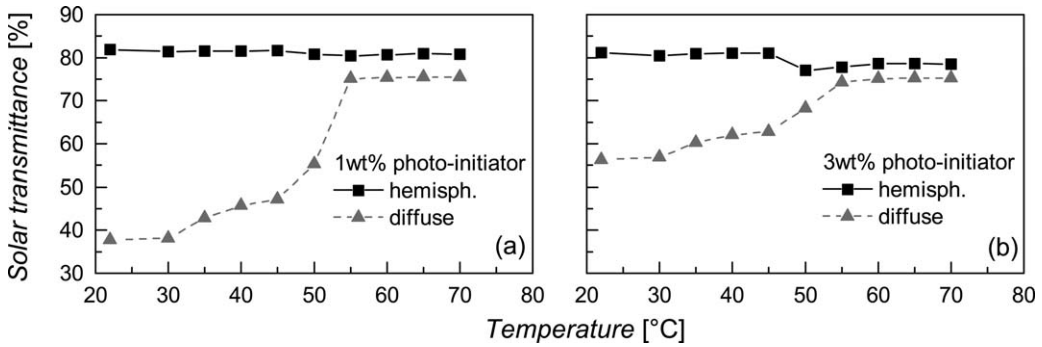

Figure 8. Solar hemispheric (square) and diffuse (triangle) transmittance of TSFD formulated with reactive diluent OTA and either (a) 1 wt % or (b) 3 wt % photo-bleaching photo-initiator and irradiated with Universal-UV-lamp after storage at room temperature (treatment RT).

function of temperature. For layer M7A1-OTA-p1-RT-0.008 solar hemispheric transmittance of 81.9 and 80.8% were evident at ambient conditions and 70°C, respectively. Diffuse transmittance increased from 37.7 to 75.5%. Layer M7A1-OTA-p3-RT-0.008 exhibited a solar hemispheric transmittance of 81.2 and 78.5% at ambient conditions and 70°C, respectively. Diffuse transmittance increased from 56.2 to 75.2%. Thus, by lowering irradiation intensity and dose a significant improvement of light shielding efficiency was achieved. This is correlating well with layer morphology. Nevertheless, for optimum overheating protection performance solar hemispheric transmittances of >85% and <60% are required in the transparent and opaque state, respectively.[4] Inappropriate light-shielding efficiency achieved for layers M7A1-OTA-p1-RT-0.008 and M7A1-OTA-p3-RT-0.008 within the present study is attributable to inappropriate scattering domain size. Hence, future work should focus on optimizing scattering domain size. As already pointed out in a preceding study,[18] adjustment of scattering domain size might be achieved by manipulation of surface energy of the additive by surface active substances, chemical modification of the additive, or covalent bonding for example.

SUMMARY AND CONCLUSION

In this article the effect of formulation and processing conditions on the light-shielding properties of TSFD formulated with paraffin type additive were investigated applying UV/Vis/NIR-spectrometry and microscopy. Type of reactive diluent and applied radiation dose and intensity were found to have significant effects on light shielding characteristics of TSFD formulated with conventional photo-initiator. Highest transmittance values at room temperature were obtained by utilizing reactive diluent OTA and by lowering applied irradiation dose/intensity. Nevertheless, these layers displayed an increase in solar hemispheric transmittance upon exceeding the threshold temperature, due to vacuoles formed at the perimeter of the spherical scattering domains during manufacturing.

However, further reduction of irradiation dose/intensity required application of a photo-bleaching photo-initiator in order to achieve properly cured TSFD. TSFD formulated with photo-bleaching photo-initiator displayed an increase of solar hemispheric transmittance upon heating due to vacuoles at the perimeter of the scattering domains also. Nevertheless, upon significant reduction of irradiation dose/intensity, TSFD exhibiting a transmittance reduction upon exceeding the threshold temperature were ascertained. The improvement of light-shielding efficiency was ascribed to a reduction of vacuole concentration. The reduction in vacuole concentration was attributed to a reduction of dissipative heating of matrix material and thus to a low temperature difference between matrix and additive during processing. Anyway, size of scattering domains persisted inappropriate for efficient overheating protection. Thus, future work has to focus on improvement of scattering domain size. As pointed out previously,[18] surfactants and nucleating agents might have positive effects on scattering domain size by introducing additional crystallization loci for the thermotropic additive and by probably maintaining smaller additive droplets in matrix/additive dispersions during manufacturing process.

ACKNOWLEDGMENT

This research project is funded by the State Government of Styria, Department Zukunftsfonds (Project number 5019). The efforts in determination of solar-optical properties of parts of the formulated TSFD by Astrid Rauschenbach (PCCL) and Alexander Klutz (Department Polymer Engineering and Science, University of Leoben) are gratefully acknowledged. Furthermore the authors want to acknowledge the contributions of Cytec Surface Specialities Inc. (Drogenbos, B), Sasol Wax GmbH (Hamburg, D), HDS-Chemie HandelsgesmbH (Wien, A) and BASF SE (Ludwigshafen, D).

REFERENCES

1. Nitz, P.; Hartwig, H. *Sol. Energy* **2005**, *79*, 573.
2. Seeboth, A.; Schneider, J.; Patzak, A. *Sol. Energy Mater. Sol. Cells* **2000**, *60*, 263.
3. Yao, J.; Zhu, N. *Build. Environ.* **2012**, *49*, 283.
4. Wallner, G. M.; Resch, K.; Hausner, R. *Sol. Energy Mater. Sol. Cells* **2008**, *92*, 614.
5. Nitz, P.; Wagner, A. *BINE Themeninfo* **2002**, *I/02*, 1.
6. Resch, K.; Wallner, G. M. In Proceedings of ISES Solar World Congress 2007, Solar energy and human settlement; Goswami, D. Y., Zhao, Y., Eds.; PRC: Beijing; Springer: Berlin; September 18–21, **2007**; pp 541–545.
7. Resch, K.; Wallner, G. M. *Sol. Energy Mater. Sol. Cells* **2009**, *93*, 119.
8. Resch, K.; Wallner, G. M. *Polym. Adv. Technol.* **2009**, *20*, 1163.
9. Resch, K.; Wallner, G. M.; Hausner, R. *Sol. Energy* **2009**, *83*, 1689.
10. Resch, K.; Wallner, G. M.; Lang, R. W. *Macromol. Symp.* **2008**, *265*, 49.
11. Resch, K.; Weber, A. *Berg-Huettenmaenn. Monatsh.* **2011**, *156*, 429.
12. Muehling, O.; Seeboth, A.; Haeusler, T.; Ruhmann, R.; Potechius, E.; Vetter, R. *Sol. Energy Mater. Sol. Cells* **2009**, *93*, 1510.
13. Bühler, F. S.; Hewel, M. *(EMS-Inventa AG). Ger. Pat. DE 198,41,234* C1 (**1998**).
14. DeArmitt, C.; Mc Kee, G. E. *(BASF SE). Eur Pat EP 1 985,663,*A1 (**2008**).
15. Weber, A.; Resch, K. In Conference Proceedings of the 6th ENERGY FORUM, Solar Building Skins, Bressanone, Italy, December 6–7, 2011, pp 73–77; Economic Forum, Ed.: Munich, **2011**.
16. Weber, A.; Resch, K. *J. Polym. Res.* **2012**, *19*, article no. 9888, 1.
17. Weber, A.; Resch, K. Thermotropic Glazings for Overheating Protection Part I: Material Pre-selection, Formulation and Light-Shielding Efficiency, submitted to *J. Polym. Res.*
18. Weber, A.; Schmid, A.; Resch, K. Thermotropic Glazings for Overheating Protection Part II: Morphology and Structure-Property-Relationships, submitted to *J. Polym. Res.*
19. Weber, A.; Resch, K. *Energy Procedia* **2012**, *30*, 471.

20. Nitz, P. Optische Modellierung und Vermessung thermotroper Systeme. Dissertation, Albert-Ludwigs-Universität, Freiburg i.B., August **1999**.
21. Gruber, D. P.; Winkler, G.; Weber, A.; Resch, K. Novel approach to the solution of the scattering problem in a thermotropic medium, manuscript in preparation.
22. Decker, C. *Polym. Int.* **1998**, *45*, 133.
23. Ivanov, V. V.; Decker, C. *Polym. Int.* **2001**, *50*, 113.
24. Decker, C. *Prog. Polym. Sci.* **1996**, *21*, 593.
25. Miller, G. A.; Gou, L.; Narayanan, V.; Scranton, A. B. *J. Polym. Sci. A: Polym. Chem.* **2002**, *40*, 793.
26. Decker, C.; Zahouily, K.; Decker, D.; Nguyen, T.; Viet, T. *Polymer* **2001**, *42*, 7551.
27. Decker, C. *Macromol. Rapid Commun.* **2002**, *23*, 1067.
28. Decker, C.; Moussa, K. *J. Appl. Polym. Sci.* **1995**, *55*, 359.
29. Baur, E.; Brinkmann, S.; Osswald, T. A.; Schmachtenberg, E. Saechtling-Kunststoff-Taschenbuch; Hanser: München, **2007**.
30. Schimmelpfennig, M.; Weber, K.; Kalb, F.; Feller, K.-H.; Butz, T.; Matthäi, M. In Jahrbuch für den Praktiker 2007: Handbuch für Rohstoff und Formulierung Industrie, Gewerbe und Haushalt; Ziolkowsky, B., Ed.; Verlag für chemische Industrie: Augsburg, **2007**; Vol. *50*, pp 417–429.
31. Ehrenstein, G. W. Polymer-Werkstoffe: Struktur-Eigenschaften-Anwendung; Hanser: München, **2011**.
32. Arceneaux, J. A.; Willard, K. UV&EB Chemistry and Technology. RadTech Printer's Guide. http://72.52.184.8/~radtecho/pdfs/PrinterGuideChemistry.pdf (accessed on January 10 2013).
33. Mikl, M. J. Herstellung und Charakterisierung von thermotropen Systemen mit fixierten Domänen. Diplomarbeit, Montanuniversität Leoben, Leoben, September **2010**.